Sandwich-type H2/CO2 membranes comprising of graphene oxide and sodalite crystals with adjustable morphology and size

Ge Yang, Hailing Guo, Zixi Kang, Shou Feng, Lei Zhao, Svetlana Mintova

Sandwich-type H_2/CO_2 membranes comprising of graphene oxide and sodalite crystals with adjustable morphology and size

Ge Yang [a], Hailing Guo [*a], Zixi Kang [c], Shou Feng [c], Lei Zhao [a], Svetlana Mintova[*ab]

a State Key Laboratory of Heavy Oil Processing, Key Laboratory of Catalysis, China National Petroleum Corp. (CNPC) China University of Petroleum (East China), Qingdao 266555, People's Republic of China. Email:guohl@upc.edu.cn

b Laboratoire Catalyse et Spectrochimie (LCS), Normandie University, ENSICAEN, UNICAEN, CNRS, 6 boulevard du Marechal Juin, 14050 Caen, France.

c College of Science, China University of Petroleum (East China), Qingdao, Shandong 266580, People's Republic of China.

**Corresponding Author. Email: mintova@ensicaen.fr*

Abstract

Sandwich-type membranes comprising of graphene oxide (GO) as a “bun” and sodalite (SOD) nanocrystals with different morphology and size as an inner layer were prepared. First, the SOD nanocrystals with spheroidal (size of 30 nm) and flake-like (size of 150 nm) morphology were synthesized from precursor suspensions containing the same amount of GO as a modifier but different amount of water. Second, the SOD nanocrystals with different morphology and size were deposited between two GO layers to form the sandwich-type membrane. The performance of the sandwich-type membranes in H_2/CO_2 gas separation was optimized by tuning the properties of the SOD inner layer. The membrane containing spheroidal SOD nanocrystals showed higher H_2 permeance of 4003±1965 GPU and H_2/CO_2 selectivity of 45.5±1.7 at 25 ºC in comparison to the pristine GO membrane (1642±145 GPU and H_2/CO_2 selectivity of 11.2±2.1).

Keywords

Sodalite nanocrystals, morphology control, composite membrane, gas separation

1. Introduction

Recently, graphene oxide(GO)-based composite membranes including GO/MOFs, GO/ZIFs, GO/COFs and GO/zeolite have attracted great attention due to the fact that the porous material (filler) can repair the in-plane defects and adjust the interlayer spacing between GO layers. Using GO can bring additional porosity and thus improve the efficient sieving of light gases or small ions [1-4]. Homogeneous and gap-free dispersion of porous materials including zeolites in graphene oxide remains the major challenge because of differences properties, which causes the low separation efficiency of the membranes due to the following reasons: (1) the weak interactions between GO matrix and the porous materials inevitably results in void formation, which further affects their separation efficiency, (2) the low content of porous materials weaken their performance in gas separation if the defects are still present. The GO-based sandwich-type composite membrane can be prepared by stacking layers with complementary properties in order to improve the gas separation performance. In GO-based sandwich-type composite membrane, size, morphology, arrangement and also chemical property of the active inner-layer are the key to improve their membrane separation performance. The material of the inner-layer should serve two purpose, one is to repair defects of GO layers, and other is to provide a higher selectivity based on size sieving or diffusional limitation.

Compared with the traditional method of controlling the morphology and size of porous materials (such as zeolite), the modulation synergy method is easier to implement by simple adding modulators to the reaction solution to control the size and morphology of porous materials [5-6], etc. Recently, GO with abundant oxygenic functional groups (epoxy groups, carbonyl groups, carboxyl groups and hydroxyl groups) on the edges and basal planes, has been considered to be an ideal modulator and additive; the GO has tremendous potential as 2D support towards formation of new composites [7-9]. Faceted ZSM-5 zeolite (6 μm) was synthesized via adding 5% GO sheets to the synthetic mixture, where GO sheets were more stably adsorbed on the {010} and {100} facets than on the {101} facet, resulting in c-axes oriented growth [10]. Guo synthesized Silicalite-1/GO composite (1 μm), which presented b-oriented nanosheets with three-dimensional intergrowth, resulting from the oriented array of organic template through dipole-charge interaction with GO's functional groups [11]. Another study on Silicalite-1/GO was reported by Wang, in which the particle size of the Silicalite-1 was increased from 0.6 μm to 12 μm under the assist of 10% GO as the oxygen-containing groups promoted the nucleation and growth of Silicalite-1 zeolite via favorable interaction with silica species [7]. GO sheets could completely envelop the zeolite particles and

function as physical barriers to confine zeolite growth [12]. Previous studies have confirmed that GO is a very effective modulator in the regulation of morphology, size and orientation of zeolites.

In this work, sodalite (SOD) nanocrystals (an aperture size of 2.8 Å) with different morphology and size were synthesized and used as an inner-layer for sandwich-type GO based membrane [13-14]. Firstly, the morphology of SOD nanocrystals was controlled by using GO as synthesis modifier in the presence of different amount of water (Scheme 1). The low amount of water in the synthesis mixture guaranteed GO modifier with a narrow layer spacing. As a result, ultrasmall SOD spheroidal crystals (30 nm) were synthesized using narrow GO sheets. On the other side, the higher amount of water resulted in larger GO layer spacing that can only serve as anchoring substrate for the growth of flake-like SOD crystals with dimension of 150 nm. The sandwich-type membrane showed good H_2/CO_2 separation performance compared to the pure GO membrane.

2. Experimental Section

2.1. Materials

Sodium Aluminate (Technical, anhydrous) was supplied by Sigma-Aldrich, containing 50-56% Al (Al_2O_3) and 37-45% Na (Na_2O). Sodium metasilicate pentahydrate (95%) was purchased from Aladdin. Graphene Oxide (GO) was produced by the Institute of Coal Chemistry, Chinese Academy of Sciences; the GO was pre-treated at 50 ºC for 24 h before being used in the synthesis of sodalite. Nylon (Whatman) with 0.2 μm pore size was used as a substrate for preparation of the composite membranes.

2.2. Synthesis of SOD crystals with different morphologies

The classical SOD crystals were synthesized by grinding method following the procedure: 1.53 g sodium metasilicate pentahydrate and 0.59 g sodium aluminate were mixed by grinder for 15 minutes using a mortar and pestle. The resulted mixture was thermally treated in an autoclave at 80 ºC for 4 h (Table 1).

To modify the morphology and size of SOD crystals, grapheme oxide (GO) nanosheets were added to the above mixture. SOD with spheroidal shape (sphere-SOD) and SOD with flake-like shape (flake-SOD) were synthesized by varying the water content in the precursor mixture only (Table 1). The synthesis conditions for preparation of the three types SOD crystals are summarized in Table 1. The GO used as a modifier for the synthesis of sodalite crystals (samples sphere-SOD and flake-SOD) was not removal before the preparation of membrane.

2.3. Preparation of GO/sodalite/GO sandwich-type membranes via layer-by-layer method

GO was dispersed in deionized water under ultrasonication for 2h; the concentration of the GO suspension was 0.25 mg/g. Then 1 g GO suspension (0.25 mg/g) was diluted in 49 g water and additionally treated in ultrasonic bath for 2h before deposition on the nylon substrate by vacuum filtration. Then, 5 mg of samples (SOD, sphere-SOD, flake-SOD) were dispersed into 100 g deionized water, and deposited on the top of the GO layer (second layer) by vacuum filtration. Finally, another 1 g GO suspension was deposited as a third layer on the sodalite layer. The membranes were dried at 25 ºC; the membranes prepared with SOD, sphere-SOD, flake-SOD nanocrystals as interlayer are abbreviated as GO/SOD/GO, GO/sphere-SOD/GO, and GO/flake-SOD/GO, respectively (Table 2). As a reference membrane, the pure GO was deposited in two subsequent layers by vacuum filtration using 2 g GO suspension (sample GO/GO).

2.4. Characterization

The crystallinity of the as-prepared samples was determined by powder X-ray diffraction (Bruker D8 Advance) using Cu Kα radiation (40 KV, 40 mA) in the range of 5° to 75° 2θ. The size and morphology of sodalite crystals with different morphologies as well as the thickness and homogeneity of the membranes were measured by a JEOL JSM-7900F scanning electron microscope (SEM) and a JEOL JEM-2100UHR transmission electron microscope (TEM). Fourier transform infrared spectroscopy (FTIR) spectra were recorded to study the interactions between sodalite crystals and GO; spectra were recorded using a Bruker Vertex 70V spectrometer with an average of 64 scans in the range 400-4000 cm^{-1}. The effect GO on sodalite synthesis was investigated via ^{29}Si DP NMR and ^{1}H-^{29}Si CP NMR spectroscopy; the spectra were recorded by a Bruker AVANCE III 400 MHz spectrometer. The chemical composition of sodalite crystals with different morphologies was measured by EDS-SEM using JEOL-7900F SEM and Oxford Instruments X-MaxN Energy-Dispersive Spectroscopy.

2.5. Membrane permeability test

For the gas permeability test, the membranes were placed in a stainless steel reactor at standard atmospheric pressure. The schematic diagram of measurement equipment was shown in Figure S1. One side of the membrane was exposed to gas mixtures (H_2/CO_2), and another side was perched by argon (Ar). The gas flux of feed gases was measured by a soap-film flow meter. The effective membrane area was 7.85×10^{-5} m^2, which is a circle with a diameter of 10 mm. The permeate flow tare of the test gas mixtures was analyzed by a gas chromatograph using a SHIMADZU GC-2014C.

The permeance (P_i, GPU, 1GPU= 3.3928×10^{-10} $molm^{-2}s^{-1}Pa^{-1}$) of membranes was calculated according to the following equation (1):

$$P_i = \frac{Ni}{A\Delta pi} \quad (1)$$

where N_i ($mols^{-1}$) is the permeate flow rate of component i, A (m^2) is the effective membrane area, Δpi (Pa) is the trans-membrane pressure drop of i.

The selectivity of membranes was evaluated using the separation ($\alpha_{i,j}$) calculated according to the following equation (2):

$$\alpha_{i/j} = \frac{P_i}{P_j} \quad (2)$$

where *i*, *j* represents the two components in the gas mixtures.

3. Results and Discussion

3.1. Synthesis of SOD crystals using GO modifier

The SOD crystals were synthesized using the method described in reference report [15]. The XRD pattern of the sample contains all Bragg peaks characteristics of sodalite (Figure 1 a); the high purity and crystallinity of the SOD sample are confirmed. The SOD crystals are agglomerated and with an average dimension of 250 nm (Figure 1d). This SOD sample is used as a reference. The influence of GO sheets as a modifier on the crystallization of sodalite zeolite was studied. The SOD crystals synthesized with GO sheets with narrow layer spacing (sample sphere-SOD) exhibit Bragg broad peaks with lower intensity in comparison to the pure SOD (Figure 1b). The crystal size of the sphere-SOD sample calculated by Scherrer equation, using the two most intense Bragg peaks at 14.1 ° and 24.5 ° 2θ is 28 nm, which is consistent with the SEM result (Figure 1e). This result implies that the GO sheets limit the growth of sodalite crystals. The morphology of sphere-SOD crystals tightly wrapped in graphene oxide sheet is shown by TEM (Figure S2a). After adding water in the precursor mixture for the synthesis of sample flake-SOD (Table 1), the GO sheets spacing increased weakening the besiegement with the precursor mixture (Figure S2b). The XRD pattern of the flake-SOD crystals contains intense Bragg peaks due to the presence of intergrown sodalite flakes around 150 nm (Figure 1c), which is consistent with the SEM results (Figure 1f). The GO with large spacing does not limit the growth of SOD, however increases the surface that gather silica and aluminum species together in the formation of zeolites [11]. Under increasing the synthesis time, bigger sodalite

flake like crystals with the a dimension over 200 nm are obtained (Figure S3). If only adding free water into the precursor synthesis mixture without GO, a mixed LTA and SOD phases are obtained as shown in the XRD (Figure S4).

The interactions between GO and sodalite crystals was studied by FT-IR spectroscopy. The IR spectrum of pure GO nanosheets (Figure 2a) contains bands at 3430 cm^{-1} (-OH stretch), 1734 cm^{-1} (C=O stretch), 1624 cm^{-1} (skeletal ring stretch), and 1101 cm^{-1} (C-0-C stretch) [11, 16-18]. These peaks in the spectrum of sphere-SOD are blue shifts, i.e., a shift of 6 cm^{-1} and 13 cm^{-1} for the C=O band and skeletal ring peak in sample (Figure 2b); a more significant blue shift in the flake-SOD of 7 cm^{-1}, 7 cm^{-1}, and 14 cm^{-1} for the OH stretch band, C=O stretch peak, and skeletal ring stretch peak, respectively are measured (Figure 2c). Furthermore, the C-O-C stretching mode at 1101 cm^{-1} is not present in both spectra of sphere-SOD and flake-SOD. These changes of GO characteristic peaks reveal the redistribution of the GO's surface functional groups due to the interaction between GO and sodalite crystals. The different degrees of the blue shift of the IR bands of sphere-SOD and flake-SOD samples are attributed to the diverse numbers of valid anchors. As show in the TEM images, the well-spread GO sheets ensure better contact with the flake-SOD crystals (Figure S2).

The interaction between GO and sodalite crystals was further studied by ^{29}Si NMR (Figure 3). The ^{29}Si DP NMR spectra of pure SOD, sphere-SOD and flake-SOD samples all contain a peak at -85.9 ppm, which is related to the formation of Q4, Si (4Al) species, attributing to the present of SOD (Si/Al≈1). While, all the ^{29}Si DP NMR spectra contain a shoulder at -83.5 ppm, corresponding to Q3 Si (3Al, 1X); the nature of X is confirmed by ^{1}H-^{29}Si CP NMR and the peak at -83.5 ppm is attributed to Si (3Al, 1H). Therefore, this peak is related to the amount of silanol groups in the samples. From the peak fitting, the ratio of the shoulder peak area to the total peaks area is 46.5 % (SOD), 49.4 % (sphere-SOD) and 37.5 % (flake-SOD) samples, respectively. This was in accordance with the chemical composition of the samples (Si/Al >1), where flake-SOD presents the lowest Si/Al, and sphere-SOD shows the highest Si/Al due to more defects sites of SOD with smaller particles and well developed surface area (Figure S5). This result is in the line with FT-IR, where the band at 877 cm-1 corresponding to Si-OH bending mode in the sphere-SOD sample is stronger than in the flake-SOD (Figure 2) [19].

3.2. Sandwich-type membranes

The sandwich-type membranes were prepared by layer-by-layer method, where for the inner layer sodalite crystals with different morphologies were used (Scheme S1). The effect of the SOD crystals

with different size and morphology on the structure of the membranes was investigated by SEM. The surfaces of the composite membranes are shown in Figure 4. For comparison, continuous pure GO membrane with folds on the surface is shown in Figure 4a. The sphere-SOD crystals with nanometer size in the GO/sphere-SOD/GO sandwich-type membrane is depicted in Figure 4c. The bigger flake-SOD crystals form defects in the bulk and on the surface of the GO/flake-SOD/GO membrane (Figure 4e). The sodalite crystals with larger size do not stack tightly between the GO layers. The cross-section images show the structure of the sandwich-type membranes, and more pronounce the difference in the stacking density. The pure GO membrane had the typical lamellar structure with a thickness of 0.3 μm (Figure 4b). The sandwich-type membranes have a thickness of about 3 μm (Figure 4d, f). The sphere-SOD crystals in the membrane are more tightly packed than the flake-SOD. The closely packed sodalite crystals in the GO/sphere-SOD/GO membrane is considered to be beneficial for defects sealing . While, the loose packing of the flake-SOD increases the free volume of the in the GO/flake-SOD/GO membrane, which would have a negative effect on selectivity but possibly will improve the permeance in gas separation.

3.3. Gas separation performance of sandwich-type membranes

The influence of the morphology and size of the sodalite crystals on membranes' permselectivity was investigated (Figure 6). As shown, the pure GO membrane exhibits 1642 ± 145 GPU hydrogen permeance with 11.2 ± 2.0 H_2/CO_2 selectivity factor, which comes from the layer spacing sieving and defects transportation behavior in the pure GO membrane. The H_2/CO_2 separation performance of the sandwich-type membrane is greatly improved by the incorporation of sphere-SOD nanocrystals. The GO/sphere-SOD/GO membrane shows the highest selectivity factor (45.4±1.7) with lowest CO_2 permeance (88±1 GPU) that is due to the healing of the defects and high stacking density. While, the hydrogen permeance up to 4003±197 GPU for the GO/sphere-SOD/GO membrane is measured resulting from the introduction of sphere-sodalite particles. The mechanism of the concurrent improvement of H_2/CO_2 selectivity and hydrogen permeance is shown in Scheme 2. In contrast, GO/flake-SOD/GO membrane exhibits high hydrogen and carbon dioxide permeance with unimproved selectivity. The addition of flake-SOD crystals only increases the free volume in the membrane, while the loose packing of the cryatsls and abundant amount of defects result in unimproved selectivity compared to pure GO membrane.

The permeance of the sandwich-type membranes was also studied using a single gas (Figure 6, Table S3). The molecules with bigger kinetic diameter (d_{N2} is 0.364 nm and D_{CH4} is 0.38 nm) have higher permeance than CO_2, thus revealing that the improvement of gas separation performance come

from the synergistic effect of GO's defects reduction and the presence of nanosized SOD crystals. The higher CO_2 diffusion rate was ascribed to the stronger attraction of the functional groups of GO to polar molecules than non-polar such as N_2 , CH_4.

The thermal stability and cycling of GO/sphere-SOD/GO membrane were studied (Figure 7). The temperature increases from 25 ºC to 100 ºC on the H_2/CO_2 mixed gas separation performance of the GO/sphere-SOD/GO membrane resultes in an increase of permeance of both H_2 and CO_2 (Figure 7a). The CO_2 permeance increases faster compared with H_2, leading to a reduction of the H_2/CO_2 selectivity factor from 45.4±1.7 to 17.2±0.8 (Table S2). This observation is consistent with the previous reports; more sensitive CO_2 permeance from temperature increases due to the formation of interlayer galleries at high temperature [20-21]. Therefore, it is suggested that low temperature guarantees better performance of the GO based membranes in gas separation. However, even at 100 ºC, the H_2/CO_2 selectivity of GO/sphere-SOD/GO is higher compared to pure GO membrane. Ten subsequent cycles for GO/sphere-SOD/GO sandwich membrane for H_2/CO_2 separation at 25 ºC were performed. No significant degradation of the membrane performance is detected, indicating the satisfactory stability in the long run use (Figure 7b).

The performance of the sandwich-type membrane in hydrogen separation is presented by Robeson upper boundary [22]. As shown in Figure 8 and Table S4, the sandwich-type GO/sphere-SOD/GO membrane in this work exhibites higher H_2/CO_2 selectivity with relative high H_2 permeance compared to pure GO membranes, indicating that sodalite crystals with proper morphology could seal defects effectively.

4. Conclusions

Graphene oxide with different amount of water in the precursor mixtures was used as a modifier to control the morphology and size of the sodalite crystals. Two types SOD crystals with spheroidal and flake-like morphologies and size of 30 nm and 150 nm were synthesized. The sodalite nanocrystals and graphene oxide were then used for the preparation of sandwich-type membranes The nanosized sphere-SOD crystals improved significantly the performance of the membrane in H_2/CO_2 mixed gas separation compared with the pristine GO membrane. The high selectivity of the sandwich-type membrane is due to the sealing of defects of GO layers and improving the stacking between sodalite nanocrystals and GO. The high stability of the membrane at elevated temperature and after 10 subsequent test cycles was demonstrated. The performance of the sandwich-type

membrane could be further optimize by controlling the thickness, number of layers deposited, and packing of crystals in the inner-layer.

Conflicts of interest

There are no conflicts to declare.

Acknowledgements

The authors gratefully acknowledged funding from Thousand Talents Program for Foreign Experts (WQ20152100284), the French-China Science Foundation (FFCSA), the National Natural Science Foundation of China (Grant No. 21975285, No. U1862118 and No. 18CX05018A), and the Sino-French LIA “Zeolite”.the International Associated Laboratory (LIA)-Zeolites.

References

[1] X. Wang, C. Chi, J. Tao, Y. Peng, S. Ying, Y. Qian, J. Dong, Z. Hu, Y. Gu, D. Zhao, Improving the hydrogen selectivity of graphene oxide membranes by reducing non-selective pores with intergrown ZIF-8 crystals, CHEM. COMMUN. (Cambridge, England), 52 (2016) 8087-8090.

[2] Y. Hu, J. Wei, Y. Liang, H. Zhang, X. Zhang, W. Shen, H. Wang, Zeolitic Imidazolate Framework/Graphene Oxide Hybrid Nanosheets as Seeds for the Growth of Ultrathin Molecular Sieving Membranes, ANGEW. CHEM. INT. EDIT., 55 (2016) 2048-2052.

[3] A. Huang, Q. Liu, N. Wang, Y. Zhu, J. Caro, Bicontinuous Zeolitic Imidazolate Framework ZIF-8@GO Membrane with Enhanced Hydrogen Selectivity, J. AM. CHEM. SOC., 136 (2014) 14686-14689.

[4] Z. Kang, S. Wang, R. Wang, H. Guo, B. Xu, S. Feng, L. Fan, L. Zhu, W. Kang, J. Pang, H. Sun, X. Du, M. Zhang, D. Sun, Sandwich membranes through a two-dimensional confinement strategy for gas separation, Mater. Chem. Front., 2 (2018) 1911-1919.

[5] Z. Li, R.S. Bownan, Sorption of Perchloroethylene by Surfactant-Modified Zeolite as Controlled by Surfactant Loading, ENVIRON. SCI. TECHNOL., 32 (1998) 2278-2282.

[6] S.J. Turner, J. Chen, A.M.Z. Slawin, W. Zhou, New mechanism for the nucleation and growth of large zeolite X crystals in the presence of triethanolamine, CHEM. COMMUN. (Cambridge, England), 55 (2019) 862-865.

[7] D. Li, L. Qiu, K. Wang, Y. Zeng, D. Li, T. Williams, Y. Huang, M. Tsapatsis, H. Wang, Growth of zeolite crystals with graphene oxide nanosheets, CHEM. COMMUN. (Cambridge, England), 48 (2012) 2249.

[8] L. Gongping, J. Wanqin, X. Nanping, Graphene-based membranes, CHEM. SOC. REV., 44 (2015) 5016-5030.

[9] R.K. Joshi, S. Alwarappan, M. Yoshimura, V. Sahajwalla, Y. Nishina, Graphene oxide: the new membrane material, APPL. MATER. TODAY., 1 (2015) 1-12.

[10] H. Li, X. Liu, S. Qi, L. Xu, G. Shi, Y. Ding, X. Yan, Y. Huang, J. Geng, Graphene Oxide Facilitates Solvent-Free Synthesis of Well-Dispersed, Faceted Zeolite Crystals, ANGEW. CHEM. INT. EDIT., 56 (2017) 14090-14095.

[11] D. He, X. Ni, Y. Zhang, J. Zhang, Z. Zeng, M. Qi, B. Peng, X. Guo, Synthesis of b-Oriented MFI Nanosheet with High-aspect Ratio by Suppressing Intergrowth with 2D GO Nanosheet, CRYSTENGCOMM., 19 (2017).

[12] D.W. Kim, H. Han, H. Kim, X. Guo, M. Tsapatsis, Preparation of a graphene oxide/faujasite composite adsorbent, MICROPOR. MESOPOR. MAT., 268 (2018) 243-250.

[13] W. Fan, K. Morozumi, R. Kimura, T. Yokoi, T. Okubo, Synthesis of Nanometer-Sized Sodalite Without Adding Organic Additives, LANGMUIR., 24 (2008) 6952-6958.

[14] S. Lee, Y. Son, A. Julbe, J. Choy, Vacuum seeding and secondary growth route to sodalite membrane, THIN. SOLID. FILMS., 495 (2006) 92-96.

[15] L. Ren, Q. Wu, C. Yang, L. Zhu, C. Li, P. Zhang, H. Zhang, X. Meng, F. Xiao, Solvent-Free Synthesis of Zeolites from Solid Raw Materials, J. AM. CHEM. SOC., 134 (2012) 15173-15176.
[16] H. Yang, N. Wang, L. Wang, H. Liu, Q. An, S. Ji, Vacuum-assisted assembly of ZIF-8@GO composite membranes on ceramic tube with enhanced organic solvent nanofiltration performance, J. MEMBRANE. SCI., 545 (2018) 158-166.
[17] Y. Li, H. Liu, H. Wang, J. Qiu, X. Zhang, GO-guided direct growth of highly oriented metal–organic framework nanosheet membranes for H2/CO2 separation, CHEM. SCI., 9 (2018) 4132-4141.
[18] M. Khatamian, B. Divband, F. Farahmand-zahed, Synthesis and characterization of Zinc (II)-loaded Zeolite/Graphene oxide nanocomposite as a new drug carrier, MAT. SCI. ENG. C-MATER., 66 (2016) 251-258.
[19] W. Fan, K. Morozumi, R. Kimura, T. Yokoi, T. Okubo, Synthesis of Nanometer-Sized Sodalite Without Adding Organic Additives, LANGMUIR., 24 (2008) 6952-6958.
[20] C. Chi, X. Wang, Y. Peng, Y. Qian, Z. Hu, J. Dong, D. Zhao, Facile Preparation of Graphene Oxide Membranes for Gas Separation, CHEM. MATER., 28 (2016) 2921-2927.
[21] L. Hang, S. Zhuonan, Z. Xiaojie, H. Yi, L. Shiguang, M. Yating, H.J. Ploehn, B. Yu, Y. Miao, Ultrathin, molecular-sieving graphene oxide membranes for selective hydrogen separation, SCIENCE., 342 (2013) 95-98.
[22] L.M. Robeson, The upper bound revisited, J. MEMBRANE. SCI., 320 (2008) 390-400.
[23] A.F.M. Ibrahim, F. Banihashemi, Y.S. Lin, Graphene oxide membranes with narrow inter-sheet galleries for enhanced hydrogen separation, CHEM. COMMUN. (Cambridge, England), 55 (2019) 3077-3080.
[24] K. Huang, J. Yuan, G. Shen, G. Liu, W. Jin, Graphene oxide membranes supported on the ceramic hollow fibre for efficient H 2 recovery, CHINESE. J. CHEM. ENG., 25 (2017) 752-759.
[25] A. Ibrahim, Y.S. Lin, Gas permeation and separation properties of large-sheet stacked graphene oxide membranes, J. MEMBRANE. SCI., 550 (2018) 238-245.
[26] K. Guan, J. Shen, G. Liu, J. Zhao, H. Zhou, W. Jin, Spray-evaporation assembled graphene oxide membranes for selective hydrogen transport, SEP. PURIF. TECHNOL., 174 (2017) 126-135.

Schemes

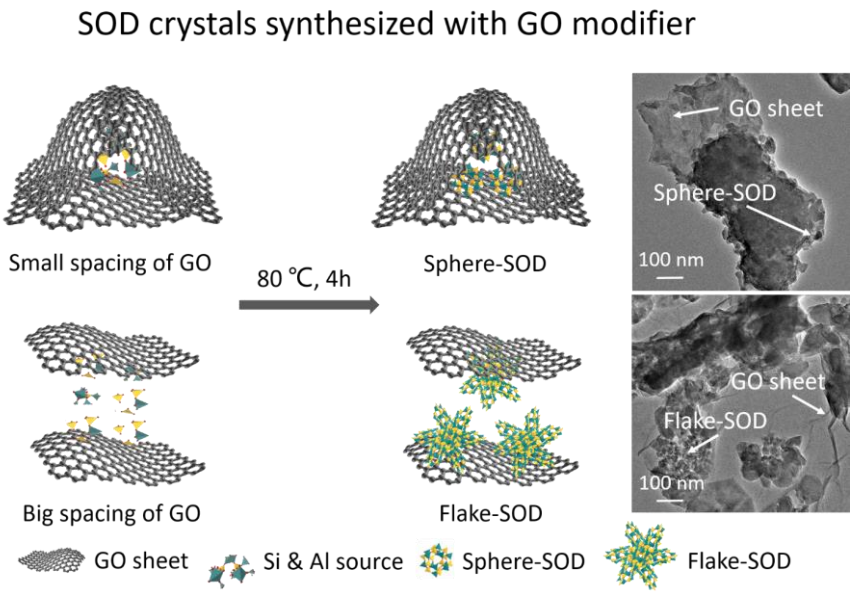

Scheme 1. Schematic presentation of the effect of GO modifier with different layer spacing on morphology and size of SOD crystals. Upper part: small spacing of GO resulted in the synthesis of spheroidal SOD with a size of 30 nm; Bottom part: large spacing of GO resulted in the synthesis of flake-like SOD with a size of 150 nm.

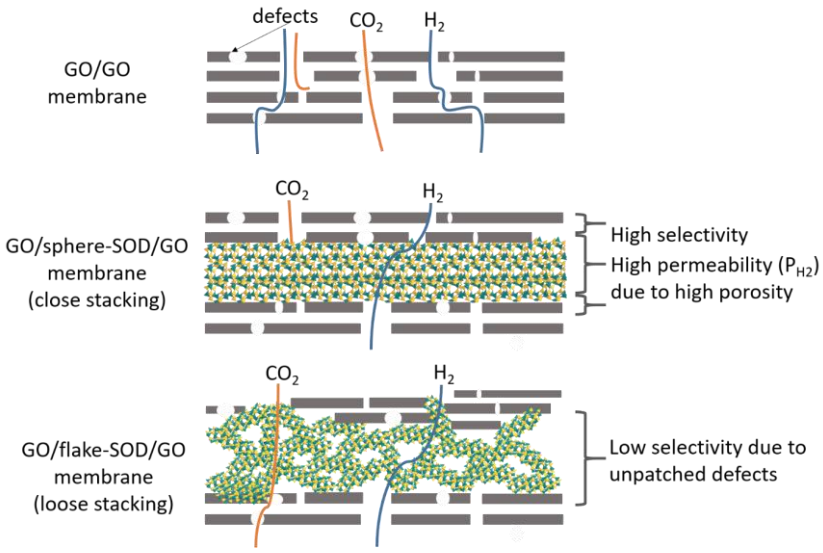

Scheme 2. Schematic diagram of gas separation mechanism of pure GO, and sandwich-type GO/sphere-SOD/GO and GO/flake-SOD/GO membranes

Tables

Table 1. Synthesis conditions used for sodalite crystals with different morphologies

Sample	Molar mixture composition SiO_2:Al_2O_3:Na_2O:H_2O	Water/g	GO/mg	Synthesis time/h
SOD	2.2:1:3.5:11.1	0	0	4
sphere-SOD	2.2:1:3.5:11.1	0	21	4
flake-SOD	2.2:1:3.5:50.8	2.213	21	4

Table 2. Preparation conditions of GO-based sandwich-type membranes via layer-by-layer method with different sodalite crystals as interlayer

Membranes	First layer	Second layer	Third layer
GO/SOD/GO	0.25 mg GO	5 mg SOD	0.25 mg GO
GO/sphere-SOD/GO	0.25 mg GO	5 mg sphere-SOD	0.25 mg GO
GO/flake-SOD/GO	0.25 mg GO	5 mg flake-SOD	0.25 mg GO
GO/GO	0.25 mg GO	--	0.25 mg GO

Figures

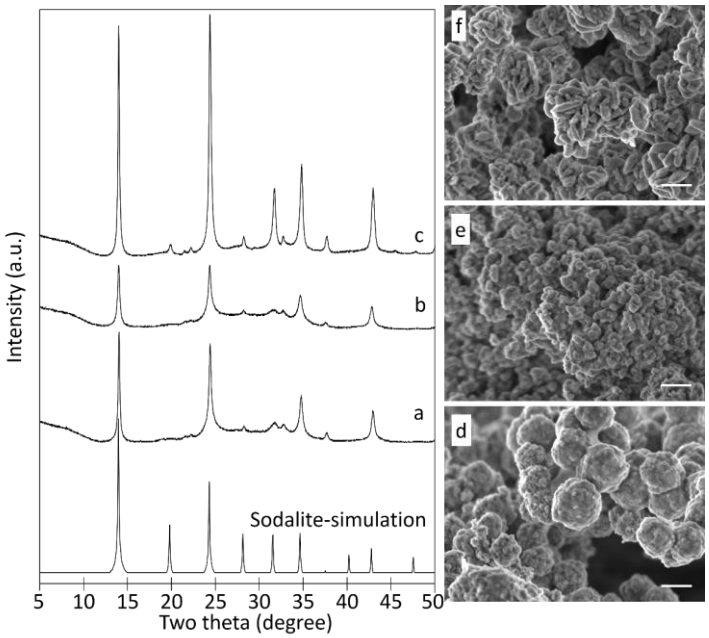

Figure 1. XRD patterns of (a) pure SOD, (b) sphere-SOD, and (c) flake–SOD samples; .SEM images of (d) pure SOD, (e) sphere-SOD, and (f) flake-SOD (Scale bar: 200 nm)

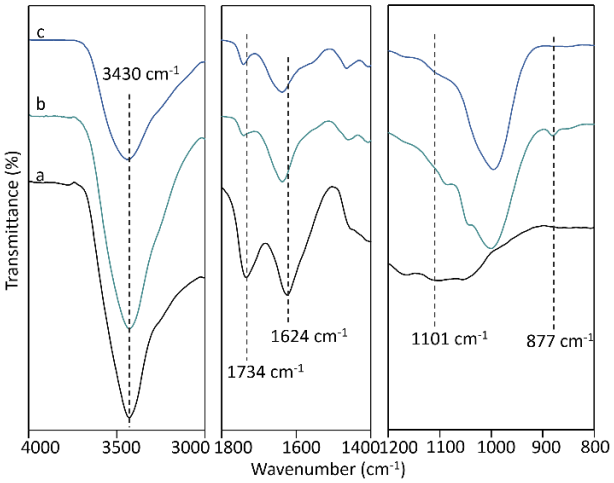

Figure 2. FT-IR spectra of (a) graphene oxide (GO), (b) sphere-SOD and (c) flake-SOD samples

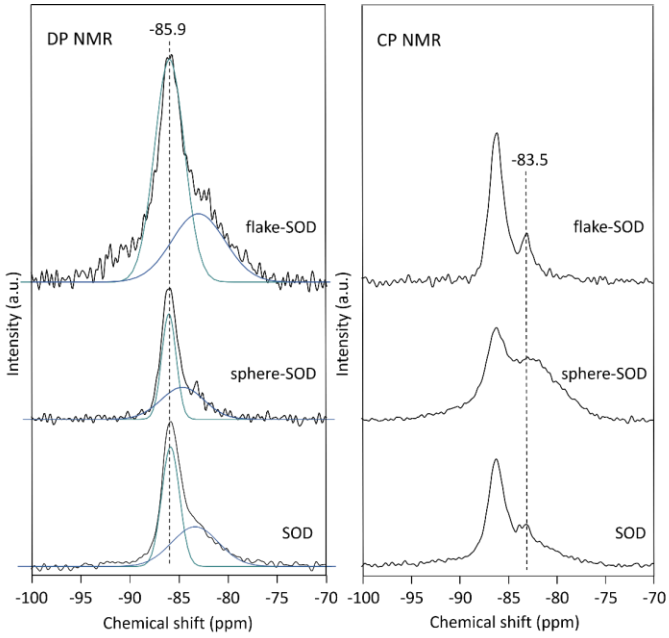

Figure 3. ^{29}Si DP NMR spectra (left) with peak fitting and ^{1}H-^{29}Si CP NMR (right) spectra of SOD, sphere-SOD and flake-SOD samples

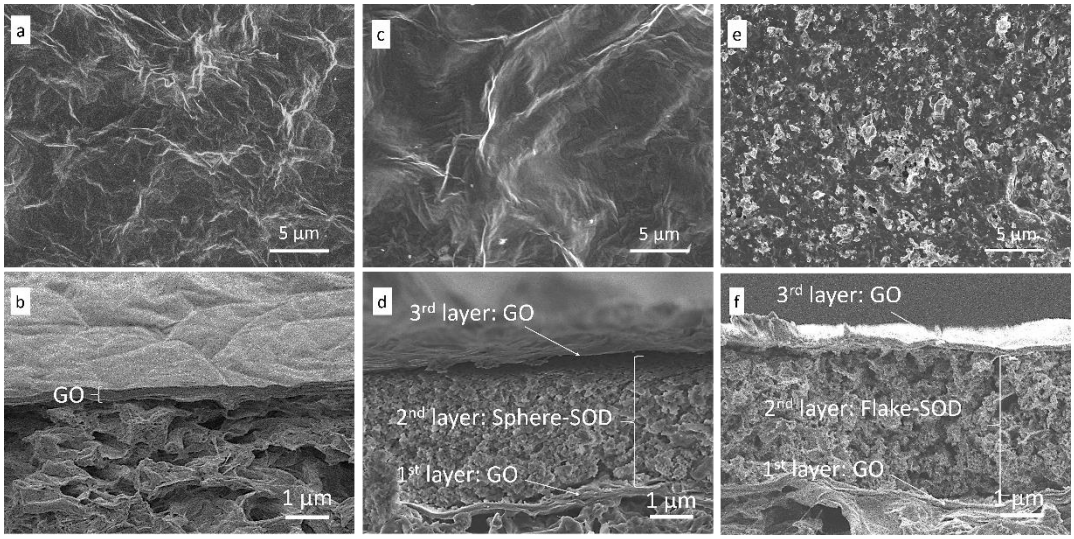

Figure 4. Top-view SEM images and cross-section SEM photos of (a, b) pure GO membrane, and (c, d) GO/sphere-SOD/GO, and (e, f) GO/flake-SOD/GO membranes

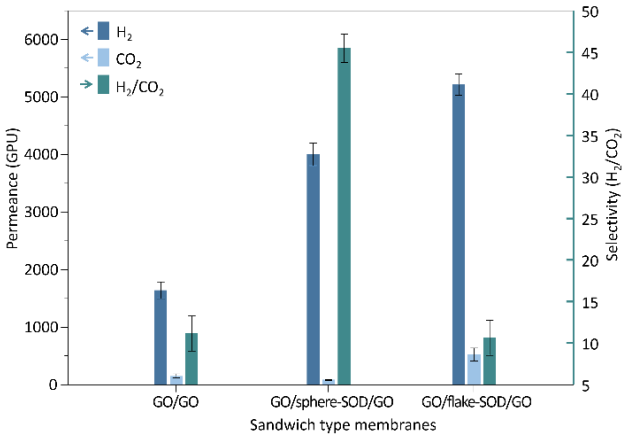

Figure 5. H_2/CO_2 gas separation performances of pure GO membrane (GO/GO), and sandwich-type GO/sphere-SOD/GO, GO/flake-SOD/GO membranes at 25 ºC

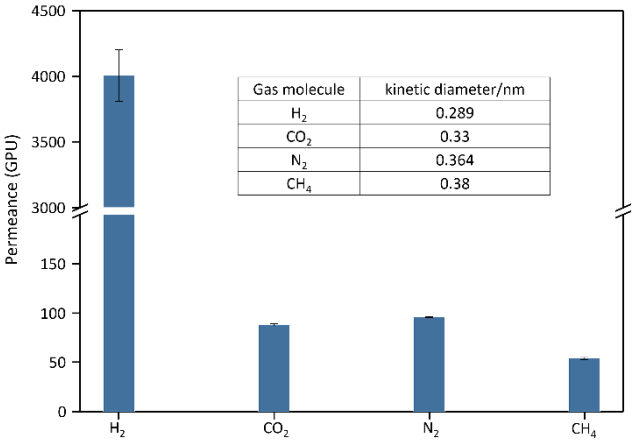

Figure 6. Single gas permeance of GO/sphere-SOD/GO membrane at 25 ºC

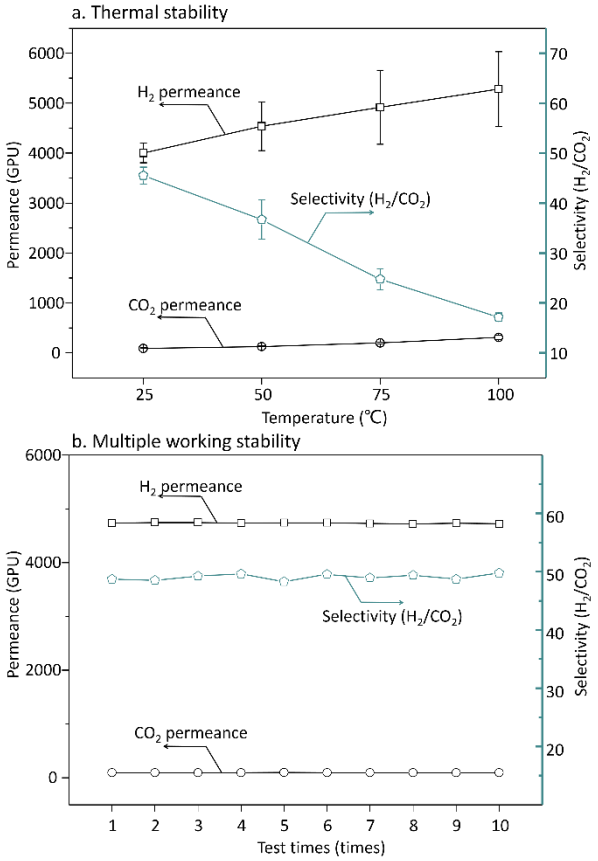

Figure 7. Permeance of GO/sphere-SOD/GO sandwich-type membrane in H_2/CO_2 mixed gas separation under (a) temperature increase from 25 ºC to 100 ºC and (b) in 10 subsequent cycles at 25 ºC

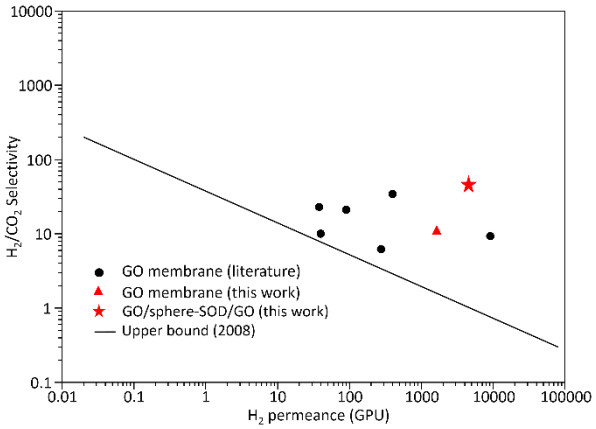

Figure 8. The relationship between H_2 permeance and H_2/CO_2 selectivity of sandwich-type GO/sphere-SOD/GO membrane compared with pure GO membranes reported in the literatures [1-2, 23-26]. The upper bound line of H_2/CO_2 is plotted according to Robeson's research [22]